

## MARCS: MODEL STELLAR ATMOSPHERES AND THEIR APPLICATION TO THE PHOTOMETRIC CALIBRATION OF THE *SPITZER SPACE TELESCOPE* INFRARED SPECTROGRAPH (IRS)

L. DECIN,<sup>1,2</sup> P. W. MORRIS,<sup>3</sup> P. N. APPLETON,<sup>3</sup> V. CHARMANDARIS,<sup>4</sup> L. ARMUS,<sup>3</sup> AND J. R. HOUCK<sup>4</sup>

Received 2004 March 26; accepted 2004 May 27

### ABSTRACT

We describe state-of-the-art MARCS-code model atmospheres generated for a group of A dwarf, G dwarf, and late-G to mid-K giant standard stars, selected to photometrically calibrate the *Spitzer Space Telescope* Infrared Spectrograph (IRS) and compare the synthetic spectra to observations of HR 6688, HR 6705, and HR 7891. The general calibration processes and uncertainties are briefly described, and the differences between various templated composite spectra of the standards are addressed. In particular, a contrast between up-to-date model atmospheres and previously published composite and synthetic spectra is illustrated for wavelength ranges around  $8\ \mu\text{m}$  (where the SiO  $\Delta v = 1$  band occurs for the cooler standards) and  $\lambda \geq 20\ \mu\text{m}$ , where the use of the Engelke function will lead to increasingly large discrepancies as a result of the neglect of gravity in cool stars. At this point, radiometric requirements are being met, absolute flux calibration uncertainties ( $1\ \sigma$ ) are  $\sim 20\%$  in the Short-High and Long-High data and  $\sim 15\%$  in the Short-Low and Long Low data, and order-to-order flux uncertainties are  $\sim 10\%$  or less. Iteration between the MARCS model atmosphere inputs and the data processing will improve the S/N ratios and calibration accuracies.

*Subject headings:* infrared: stars — instrumentation: detectors — instrumentation: spectrographs — methods: data analysis — stars: atmospheres — techniques: spectroscopic

*Online material:* color figures

### 1. INTRODUCTION

The scientific interpretation and modeling of the spectra produced by the Infrared Spectrograph<sup>5</sup> (IRS; Houck et al. 2004) on board the *Spitzer Space Telescope* (Werner et al. 2004) require accurate spectrophotometric calibrations, which depend upon stars with well-known environmental and atmospheric properties. We have a unique opportunity to use the state-of-the-art MARCS code, developed by the Uppsala group (Gustafsson et al. 1975) and modified substantially in the numerical methods and input line and continuous opacities, to compute synthetic spectra of the IRS standard stars. The iteration between stellar models and instrument calibrations has been described by Decin et al. (2000, 2003a, 2003b, 2003c), with applications to calibrations of the Short Wavelength Spectrometer (SWS) on board the *Infrared Space Observatory* (ISO).

In this paper we describe the synthetic spectra based on the MARCS code model atmospheres tailored to a set of standard stars that are relied upon for the photometric calibration of the IRS. We overview the calibration strategy and summarize the primary IRS stellar standards. The latest generation model

spectra of these stars are discussed, presented in comparison to IRS spectra of three standards. We finally contrast our synthetic spectrum for  $\gamma$  Dra (K5 III) with widely available Kurucz model and composite spectra and summarize the current photometric uncertainties.

### 2. THE IRS PHOTOMETRIC CALIBRATION SCHEME

The basic strategy for photometrically calibrating IRS spectroscopy has been outlined by Morris et al. (2003). Each spectral order in the Short-Low and Long-Low (SL and LL, respectively;  $\lambda/\Delta\lambda \simeq 70\text{--}140$ ) long-slit spectrographs, and the Short-High and Long-High (SH and LH, respectively;  $\lambda/\Delta\lambda \simeq 700$ ) echelle spectrographs, is individually calibrated by processing data from fine spectral maps of standard stars into a single two-dimensional image plane and dividing the signature of the celestial source by means of the synthetic spectra. Ideally, the spectral flat field for each array is determined by a weighted mean of flats individually derived from different stars. The resultant flat field is then applied to observations of other standards, and the spectral extractions are analyzed to determine the flux conversion coefficients (electrons per second to janskys) and polynomial “tuning” coefficients to correct for the effects of diffraction losses on point source observations, and systematic low-frequency residual errors from the flat-fielding. Initially, only sparse spectral maps of the calibration stars could be acquired, and they depended on zodiacal light observations to spatially fill in the orders.<sup>6</sup> Because of the relatively low zodiacal fluxes (in SH, LH, and SL second-order), the effects of PSF under-sampling, and space weather on the detectors, exhaustive observations of the standard stars continue to be carried out in

<sup>1</sup> Department of Physics and Astronomy, University of Leuven, Celestijnenlaan 200B, B-3001 Leuven (Heverlee), Belgium; leen.decin@ster.kuleuven.ac.be.

<sup>2</sup> Postdoctoral Fellow of the Fund for Scientific Research, Flanders.

<sup>3</sup> *Spitzer* Science Center, IPAC, California Institute of Technology, MC 220-6, 1200 East California Boulevard, Pasadena, CA 91125.

<sup>4</sup> Astronomy Department, Cornell University, 106 Space Sciences Building, Ithaca, NY 14853.

<sup>5</sup> The IRS was a collaborative venture between Cornell University and Ball Aerospace Corporation funded by NASA through the Jet Propulsion Laboratory and the Ames Research Center. The *Spitzer Space Telescope* is operated by the Jet Propulsion Laboratory, California Institute of Technology, under NASA contract 1407. Support for this work was provided by NASA through an award issued by JPL/Caltech.

<sup>6</sup> The zodiacal light itself is unreliable in the spectral dimension because of the likely presence of solid state features and latitudinal variations in dust temperature and grain properties (Reach et al. 2003).

TABLE 1  
 IRS PHOTOMETRIC CALIBRATION STARS AND DERIVED  $T_{\text{eff}}$  AND  $\log g$ 

Source	Spectral Type	Calibration <sup>a</sup>	Range <sup>b</sup>	$T_{\text{eff}}$ (K)	$\log g$ (cm s <sup>-2</sup> )
HR 6688.....	K2 III	P	SH, LH	4465 (50) <sup>c</sup>	2.17 (0.19) <sup>f</sup>
HR 7310.....	G9 III	P	[SH], [LH]	4830 (50) <sup>c</sup>	2.58 (0.06) <sup>f</sup>
HR 2194.....	A0 V	P	SL1, SL2	10325 (240) <sup>d</sup>	4.09 (0.08)
HR 7341.....	K1 III	P	LL2	4570 (50) <sup>c</sup>	2.46 (0.08)
HR 7950.....	A1.5 V	S	SL1, SL2	9060 (120) <sup>d</sup>	3.51 (0.08) <sup>f</sup>
HR 7891.....	A0 V	S	SL1, SL2	10170 (120) <sup>d</sup>	4.07 (0.07) <sup>f</sup>
HR 6705.....	K5 III	S	SH, LH	3980 (50) <sup>c</sup>	1.06 (0.09) <sup>f</sup>
HR 6606.....	G9 III	S	All	4975 (50) <sup>c</sup>	2.90 (0.07)
HR 2491.....	A1 V	T	SH, LH	10240 (120) <sup>d</sup>	4.39 (0.07) <sup>f</sup>
HD 105.....	G0 V	T	All	5930 (70) <sup>c</sup>	4.31 (0.11) <sup>g</sup>

NOTE.—Uncertainties are in parentheses (cf. eq. [18] in Decin et al. 2000).

<sup>a</sup> Calibration types: (P) principal, (S) secondary, (T) test case. Principal standards are observed to derive flat fields and absolute flux calibration; secondary standards, which may have limited visibilities or less certain stellar parameters, are observed to verify or further refine the calibrations.

<sup>b</sup> Entries refer to the IRS modules, as follows: SL1, 7.5–14.5  $\mu\text{m}$ ; SL2, 5.3–7.5  $\mu\text{m}$ ; LL1, 19.5–38.0  $\mu\text{m}$ ; LL2, 14.0–21.3  $\mu\text{m}$ ; SH, 9.9–19.6  $\mu\text{m}$ ; LH, 18.7–37.2  $\mu\text{m}$ . Parentheses denote where calibration stars may be used only over certain ranges of the module.

<sup>c</sup> Derived from  $(V - K)$ .

<sup>d</sup> Derived from  $(V - I)$ .

<sup>e</sup> Derived from  $(B - V)$ -temperature relation of Flower (1996).

<sup>f</sup> Using  $[\text{Fe}/\text{H}]$  from Cayrel de Strobel et al. (1997).

<sup>g</sup> Using  $[\text{Fe}/\text{H}]$  from the *uvby*- $\beta$ -metallicity relation of Schuster & Nissen (1989).

order to meet the radiometric requirement of 5%. The details of the stellar atmosphere models are especially important at this stage.

Table 1 summarizes the stars that have been selected and observed during SV and in IRS Science campaigns for the purposes of photometrically calibrating IRS spectroscopy. The stars were chosen in the prelaunch preparatory phase, to meet (as closely as possible) specific criteria on the availability of observational data to make reasonable estimates of the stellar parameters (described in the next section), their environments, and absence of chromospheric activity, circumstellar dust shell or disk, multiplicity, or peculiar spectral activity. The IRS operating at low resolution is  $\sim 300$  times more sensitive than SWS was at 10  $\mu\text{m}$ , and consequently the fainter standard stars may meet the aforementioned requirements to a lesser extent than stars in the *ISO* calibration programs. We make use of observations from the *ISO* ground-based preparatory program (Hammersley et al. 1998; Hammersley & Jourdain de Muizon 2003) and detailed theoretical work where possible. In particular, HR 6688, HR 6705, HR 7310, and HR 2491 in Table 1 have been previously modeled by Decin et al. (2003a, 2003c) using ground-based and 2.4–12  $\mu\text{m}$  *ISO* SWS spectroscopy.

### 3. REFERENCE SPECTRAL ENERGY DISTRIBUTIONS: MARCS SYNTHETIC SPECTRA

A new set of theoretical reference spectral energy distributions (SEDs) has been calculated using the MARCS and TURBOSPECTRUM code (see Gustafsson et al. 1975, Plez et al. 1992, and further updates), using the same physical input parameters of atomic and molecular equilibrium constants, solar abundances, continuous opacity sources, etc., as the ones described by Decin (2000). For line opacities in the IRS spectral range, a database of infrared lines with atomic and molecular transitions (CO, SiO, H<sub>2</sub>O, OH, NH, HF, HCl, CH, and NO) has been prepared. References and discussion of the inputs can be found in Decin (2000).

The computed theoretical atmosphere model and synthetic spectrum depend on a large number of input parameters, the main ones being the effective temperature  $T_{\text{eff}}$ , the gravity  $g$ , the microturbulence, and the chemical composition. In case of a spherical symmetric geometry, one also has to provide either the mass  $M$  or the radius  $R$ . The stellar parameters as determined by Decin et al. (2003a, 2003c) for stars in common with the *ISO* SWS calibrators may be adopted. However, since we aim to set up a spectral response calibration independently, we prefer to make initial estimates of  $T_{\text{eff}}$  and  $\log g$  (cm s<sup>-2</sup>) from photometric colors (see below). Since almost no information is available for the microturbulence  $\xi_r$ , a value of 2 km s<sup>-1</sup> was assumed. Nevertheless, it should be noted that since the final calibration of the *ISO* SWS relative spectral response functions (RSRF) was also based on MARCS model atmospheres, the IRS spectral response calibration and methods to iterate between the input parameters and spectroscopy (e.g., Decin et al. 2003a, 2003b, 2003c) are linked to the SWS RSRFs. Moreover, first estimates of C, N, and O abundances and the <sup>12</sup>C/<sup>13</sup>C ratio—being crucial for a correct computation of the molecular opacities in K giants—are adopted from recent analyses of the *ISO* SWS calibrators by Decin et al. (2003a). The value of  $T_{\text{eff}}$  can be calculated for K and M giants directly from  $(V - K)$ , and for A-type dwarfs from  $(V - I)$ , using (semi-) empirical color-temperature relations (e.g., Bessell et al. 1998). The  $(V - K)$  and  $(V - I)$  Johnson or Two Micron All Sky Survey (2MASS) colors were converted to the Johnson-Cousins-Glass system (Bessell & Brett 1988) and corrected for interstellar extinction using  $A_V = 0.8 \text{ mag kpc}^{-1}$  (Blackwell et al. 1990), and  $E(V - K) = A_V/1.1$  and  $A_I = 0.48A_V$  (Mathis 1990), with the distance calculated from the *Hipparcos* parallax  $\pi$ . Whenever the derived color estimates were outside the ranges specified by Bessell et al. (1998) in their Tables 7 and 8, the color-temperature relation as determined by Flower (1996) was used.

In order to estimate the gravity, one needs the radius  $R$  and the stellar mass  $M$ . The first parameter is assessed from

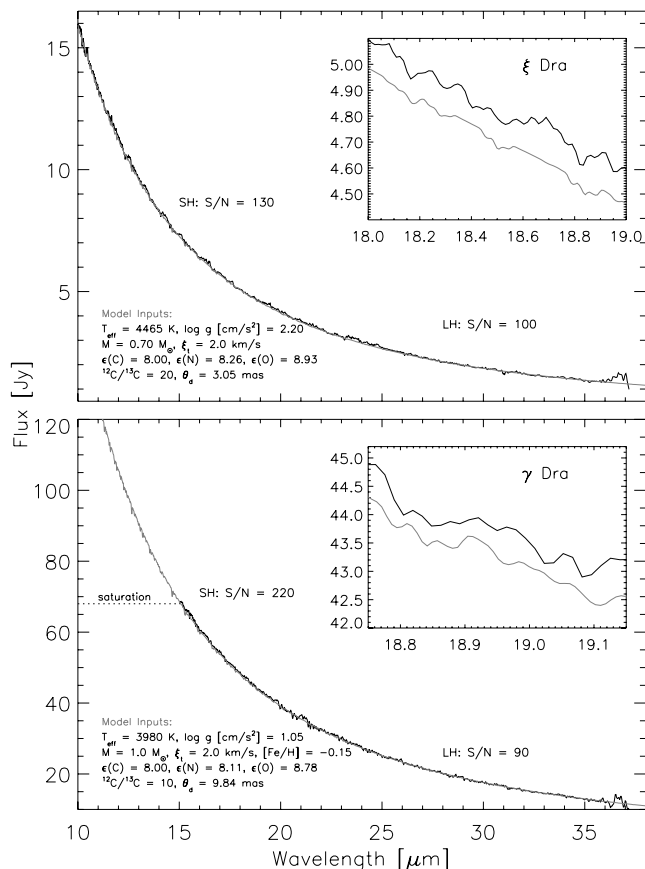


FIG. 1.—High-resolution spectra of HR 6688 (top) and HR 6705 (bottom), with the MARCS model SEDs overlotted in red. S/N ratio estimates are labeled. The insets show regions of the IRS spectrum around OH lines, compared to the model (in red, offset by  $-0.1$  Jy). [See the electronic edition of the Journal for a color version of this figure.]

( $K$ ,  $BC_K$ ,  $\pi$ ,  $T_{\text{eff}}[(V - K)_0]$ ) for K giants or ( $V$ ,  $BC_V$ ,  $\pi$ ,  $T_{\text{eff}}[(V - I)_0]$ ) for A–G dwarfs. The  $BC_K$  bolometric corrections are derived from Bessell et al. (1998) whenever appropriate, otherwise the  $BC_V$  data of Flower (1996) were used. The uncertainty on the bolometric correction is assumed to be 0.05.  $M_{\text{bol},\odot}$  is assumed to be 4.74 (Bessell et al. 1998). Mass values for the stars in our sample are estimated from evolutionary tracks with appropriate metallicity as calculated by Girardi et al. (2000). The estimated mass depends critically on the assumed metallicity, which has been adopted from literature references (see Table 1). Where no information was available, a solar metallicity was assumed. The resultant gravity for each star is listed in Table 1.

#### 4. IRS SPECTRA OF REPRESENTATIVE STANDARDS

In this section we compare reduced spectra of representative standards to their synthetic SEDs, to assess the models and calibrations. The observations have been processed to BCD products using the *Spitzer* Science Center (SSC) pipeline version S9.5.0 and were response calibrated with the latest flat fields, except for HR 6688, which was calibrated from observations of Sirius and Vega.

The comparison between the IRS spectra and the model of HR 6688 is shown in the upper panel of Figure 1. The data quality is sufficiently high to make plausible detections of spectral lines with predicted line-to-continuum ratios as low as 1% (see Fig. 1 inset displaying OH  $\Delta v = 0$  spectral features). The shape of the observed continuum is in excellent agree-

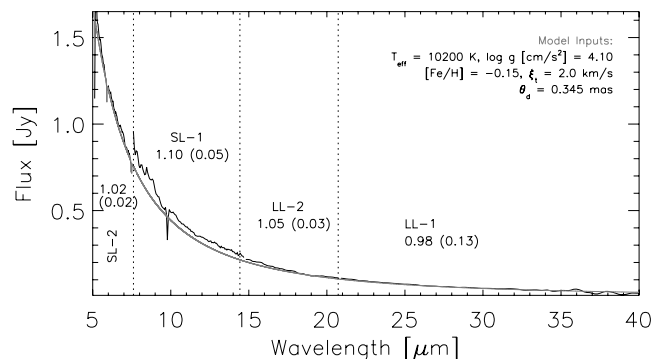


FIG. 2.—Background-corrected low-resolution spectrum of HR 7891, with the MARCS model spectrum overlotted in red. The means and standard deviations of the ratio between observations and the model SED in each spectral order are indicated. The higher spread of observed LL1 fluxes about the model is due to the 37.5–40  $\mu\text{m}$  range, where throughput response is very low, and where a soft filter cutoff allows some contamination with second-order light from  $\sim 20$   $\mu\text{m}$ . [See the electronic edition of the Journal for a color version of this figure.]

ment with the model (relying intrinsically on the accuracy of the Sirius model). The high-resolution spectrum of HR 6705, the primary flux calibrator for the *ISO* SWS, is shown in the lower panel of Figure 1. The region between 10 and 15  $\mu\text{m}$  is not plotted owing to saturation over portions of echelle orders 15–20. The remaining spectrum is calibrated with the default calibrations, that is, HR 6688-based flat fields and tuning factors. The shape of the continuum is again in excellent agreement with the model, and the inset plot again demonstrates the potential for detection of weak (molecular) spectral features, and improvements to processing methods.

The spectrum of HR 7891 plotted in Figure 2, spanning 2 orders of magnitude in flux densities, is representative of the agreement between independently calibrated low-resolution spectroscopy of this A dwarf secondary standard star, not previously observed at these wavelengths, and its MARCS model atmosphere. The background sky was subtracted with off-pointed subslits prior to spectral extraction. The ratios of the model and observations show a  $\sim 10\%$  error in the absolute flux calibration of the SL-1 portion, but otherwise excellent agreement, and they show that the star has no detectable thermal excess from a potential debris disk.

#### 5. COMPARISON WITH TEMPLATED SPECTRA

The photometric calibration schemes of the *ISO* and *Spitzer* instruments have been partly based on templated data sets, such as those constructed by M. Cohen and collaborators (e.g., Cohen et al. 2003), with both observational and theoretical components to them. The Cohen data sets can be divided into three categories: (a) a collection of absolutely calibrated photometric and spectroscopic data, merged to create a continuous spectrum with uncertainties traceable to a specific group of stars such as  $\alpha$  Tau and Vega; (b) a Kurucz model adopted at a literature consensus of  $T_{\text{eff}}$ ,  $\log(g)$ , and metallicity, then fitted to available photometry; and (c) a template constructed from a star from (a) and/or (b) with the same spectral type and scaled to the observed photometric data. Stars with the same spectral type may exhibit a different abundance pattern, affecting, e.g., the SiO band strengths and continuum levels. Products in the (a) group when available are helpful to the IRS since they rely on no theoretical assumptions, *except* for the use of an Engelke function at  $\lambda > 20$   $\mu\text{m}$ ,

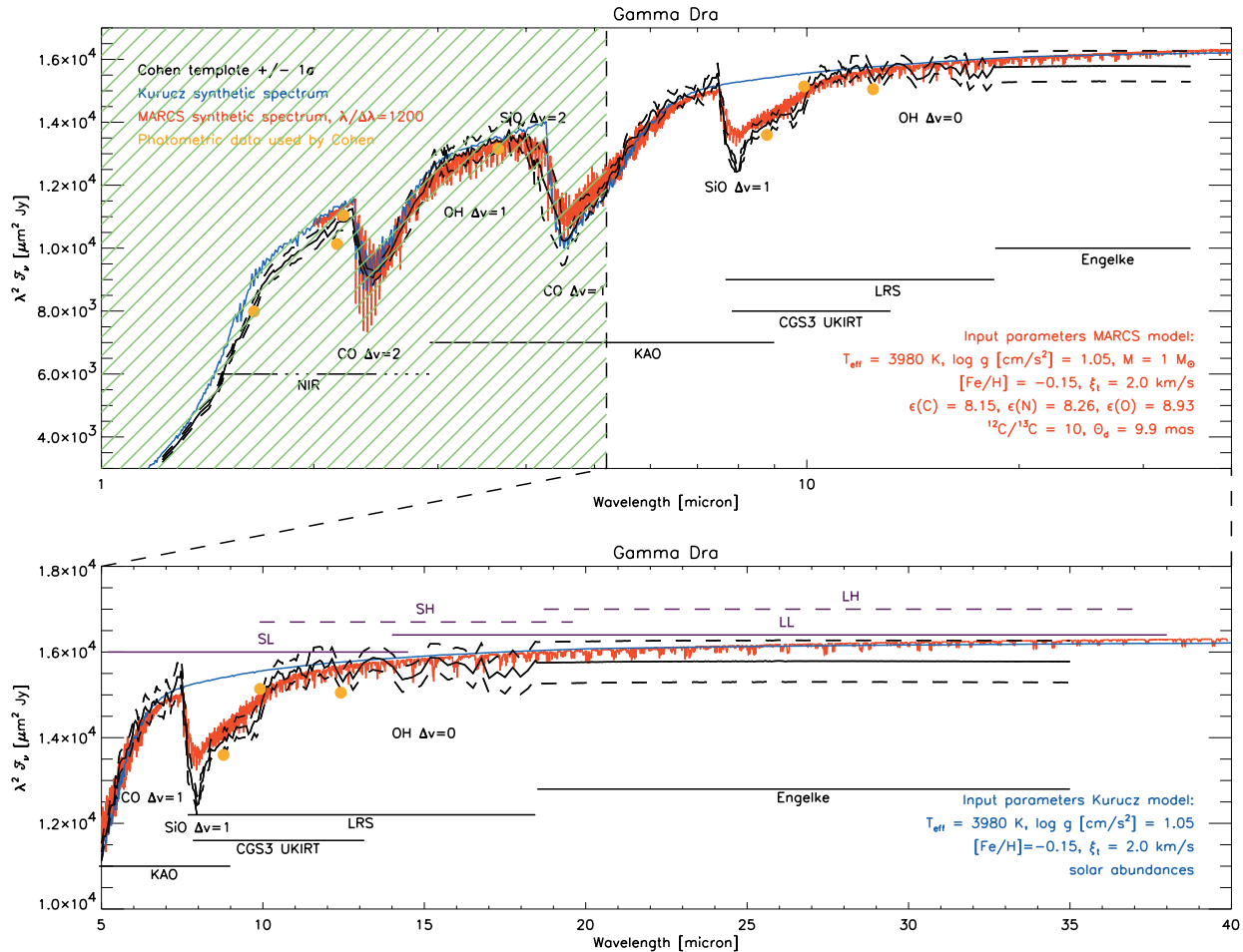


FIG. 3.—Comparison between reference SEDs of HR 6705. The composite from Cohen et al. (1996) is based on different photometric data (orange dots) and spectral fragments spliced together. The used data sets are indicated by the solid black line, and quoted uncertainty limits by the dashed lines. The input parameters for the MARCS (red) and Kurucz (blue) synthetic spectrum are indicated. In the bottom panel, the wavelength range observed by the IRS is enlarged, and the spectral coverages of SL, LL, SH, and LH are indicated.

and some products in the (c) group are also useful for instrumental checks.

For the stars listed in Table 1, we rely explicitly on the MARCS synthetic spectra for the detailed calibration analyses, noting that, while a composite is available for HR 6705 (Cohen et al. 1996), it makes use of an Engelke function extrapolation beyond  $18.5 \mu\text{m}$ , which we prefer to avoid (see next paragraph). For a wider (secondary) set of stars, which are generally too uncertain in their stellar or environmental parameters to initially justify the computational resources of MARCS modeling, we can use composite observations templated by spectral type and luminosity class, or Kurucz synthetic spectra with the understanding that they are calculated assuming a plane-parallel geometry, solar abundances (scaled to the metallicity), and a microturbulent velocity of  $2 \text{ km s}^{-1}$ , while these are all free input parameters for the MARCS atmosphere models. Note also that some of the line lists for diatomic molecules used in Kurucz models are 15 years old, are incomplete, and do not reproduce line positions very well for high  $v$  and high  $J$ . The stars of this group are typically used for trending and checks of order-to-order and module-to-module calibrations, and response to high and low flux point sources.

To illustrate these differences over the mid-IR spectral range, we show three data sets created for HR 6705 in Figure 3.

The composite constructed by Cohen et al. (1996) is plotted in black, with the photometric points and the various spectral fragments indicated. Of great importance to the IRS occurs at  $\lambda > 18.5 \mu\text{m}$ , where fluxes are approximated with the Engelke function (Engelke 1992), which offers an analytical implicit scaling of a semiempirical solar atmospheric temperature profile to differing effective temperatures. This analytical (plane-parallel) approximation should be valid for the  $2\text{--}60 \mu\text{m}$  continuum for giants and dwarfs with effective temperature  $3500 \text{ K} \leq T_{\text{eff}} \leq 6000 \text{ K}$ , where scattering of electrons from  $\text{H}^-$  dominates the continuum opacity. By fitting this function to a set of standard stars, Engelke (1992) concluded that the estimated probable error in estimated flux is  $\pm 3\%$  below  $10 \mu\text{m}$ , up to  $\pm 5\%$  in the vicinity of  $25 \mu\text{m}$ , and  $6\%$  at  $60 \mu\text{m}$ . The main spectral difference between the MARCS and Kurucz theoretical spectra is the absence of the SiO fundamental (around  $8 \mu\text{m}$ ) and first-overtone (around  $4 \mu\text{m}$ ) lines in the Kurucz spectrum. Smaller differences do occur as a result of the use of a different abundance pattern. With an extension  $d = [R(\tau_{\text{Ross}} = 10^{-5})/R(\tau_{\text{Ross}} = 1)] - 1$  being only  $3.7\%$ , the spectral differences between a plane-parallel and spherical geometry are only marginal.

The lowermost plot in Figure 3 focuses on the wavelength ranges of the SL, LL, SH, and LH modules. Two main

differences between the three data sets are of major concern for IRS calibrations: (1) around  $8 \mu\text{m}$ , where the SiO  $\Delta v = 1$  lines occur, and (2) for  $\lambda > 18.5 \mu\text{m}$ .

1. Comparison to the LRS data indicates that the abundance pattern used as input for the MARCS model and synthetic spectrum calculation should be altered, in particular the oxygen (and carbon) abundance. With the moderate resolution of IRS ( $\sim 600$ ) and the SL mode only starting around  $5 \mu\text{m}$  (being in the middle of the CO  $\Delta v = 1$  band for cool giants), it will be very difficult to constrain the stellar parameters (and in this case more specifically the oxygen abundance) from the IRS data. This situation can be avoided by relying on A dwarfs and G giants in this wavelength range.

2. At LL and LH wavelengths, we see a clear difference between the slope of the MARCS, Kurucz, and Cohen (Engelke) spectrum. With the Engelke function being a plane-parallel approximation, we have compared this function with MARCS plane-parallel spectra for  $T_{\text{eff}}$  between 3500 and 6000 K for different values of the gravity. The best agreement occurs for  $T_{\text{eff}} = 6000$  K, which is not surprising since Engelke's function is based on a scaled solar model. For lower effective temperatures, the role of the gravity becomes more important: a higher gravity results in a higher opacity (from the free-free transitions of H<sup>-</sup>), a more compact object and a smaller temperature gradient due to the requirement of flux conservation. As a consequence, the infrared continuum slope ( $\lambda > 2 \mu\text{m}$ ) is less steep for a higher gravity model. From a comparison with the MARCS continua, we may conclude that the uncertainties quoted by Engelke (1992) do not account well for the influence of gravity. For HR 6705, the difference in slopes between the MARCS model and the composite spectrum (using an Engelke function at  $\lambda > 18.75 \mu\text{m}$ ) produces *systematic* underpredictions of fluxes in the composite by 4.2% at  $30 \mu\text{m}$

and 6.3% at  $70 \mu\text{m}$ . These differences are easily within the grasp of the sensitive IRS and the MIPS detectors.

## 6. SUMMARY OF THE SPECTROPHOTOMETRIC UNCERTAINTIES

First, we estimate that for well-pointed observations of point sources, the relative photometric uncertainties within any spectral order generally meet the 5% radiometric requirement, over the spectral ranges committed to observers. The exception is the two reddest orders of LH ( $34.2\text{--}37.2 \mu\text{m}$ ), where throughput response to HR 6688 is low and will be improved with HR 6705 calibration observations by the time that this paper is published. It must also be noted that the ranges of  $14.1\text{--}15.4 \mu\text{m}$  in SL first-order and  $38\text{--}42.4 \mu\text{m}$  in LL first-order may be contaminated with light from around  $7\text{--}8$  and  $19\text{--}21 \mu\text{m}$ , respectively, because of a weakness in the transmission cutoff of the filter in the second spectral orders. The level of contamination depends on the color of the source in the slit.

The photometric performance of the IRS is very sensitive to pointing effects, owing to the sizes of the slits and the PSF widths. Combined with the effects of PSF undersampling, the absolute flux calibration is estimated at this point to be uncertain by 20% in the SH and LH data overall, and 15% in SL and LL data. Generally, order-to-order calibrations are 10% or less, for point sources in the low background (or background-corrected) limit<sup>7</sup> and well-placed in the center or nod positions of the slits. Recognizable errors can be mitigated by scaling to photometry, where available.

<sup>7</sup> The low background limit is important even for the high-resolution modules. Automatic background correction is not performed in the SSC pipeline.

## REFERENCES

- Bessell, M. S., & Brett, J. M. 1988, *PASP*, 100, 1134  
 Bessell, M. S., Castelli, F., & Plez, B. 1998, *A&A*, 333, 231  
 Blackwell, D. E., Petford, A. D., Haddock, D. J., Arribas, S., & Selby, M. J. 1990, *A&A*, 232, 396  
 Cayrel de Strobel, G., Soubiran, C., Friel, E. D., Ralite, N., & Francois, P. 1997, *A&AS*, 124, 299  
 Cohen, M., Megeath, S. T., Hammersley, P. L., Martín-Luis, F., & Stauffer, J. 2003, *AJ*, 125, 2645  
 Cohen, M., Witteborn, F. C., Carbon, D. F., Davies, J. K., Wooden, D. H., & Bregman, J. D. 1996, *AJ*, 112, 2274  
 Decin, L. 2000, Ph.D. thesis, Univ. Leuven, Belgium  
 Decin, L., et al. 2000, *A&A*, 364, 137  
 ———. 2003a, *A&A*, 400, 709  
 ———. 2003b, *A&A*, 400, 679  
 ———. 2003c, *A&A*, 400, 695  
 Engelke, C. W. 1992, *AJ*, 104, 1248  
 Flower, P. J. 1996, *ApJ*, 469, 355  
 Girardi, L., Bressan, A., Bertelli, G., & Chiosi, C. 2000, *A&AS*, 141, 371  
 Gustafsson, B., Bell, R. A., Eriksson, K., & Nordlund, Å. 1975, *A&A*, 42, 407  
 Hammersley, P. L., & Jourdain de Muizon, M. 2003, in *The Calibration Legacy of the ISO Mission*, ed. L. Metcalfe & M. F. Kessler (ESA SP-481; Noordwijk: ESA), 129  
 Hammersley, P. L., et al. 1998, *A&AS*, 128, 207  
 Houck, J., et al. 2004, *ApJS*, 154, 18  
 Mathis, J. S. 1990, *ARA&A*, 28, 37  
 Morris, P. W., Charmandaris, V., Herter, T., Armus, L., Houck, J., & Sloan, G. 2003, in *The Calibration Legacy of the ISO Mission*, ed. L. Metcalfe & M. F. Kessler (ESA SP-481; Noordwijk: ESA), 113  
 Plez, B., Brett, J. M., & Nordlund, Å. 1992, *A&A*, 256, 551  
 Reach, W. T., Morris, P., Boulanger, F., & Okumura, K. 2003, *Icarus*, 164, 384  
 Schuster, W. J., & Nissen, P. E. 1989, *A&A*, 221, 65  
 Werner, M., et al. 2004, *ApJS*, 154, 1